








# Hydrogen plasma treatment of $\beta$ -Ga<sub>2</sub>O<sub>3</sub>: Changes in electrical properties and deep trap spectra

Cite as: Appl. Phys. Lett. **115**, 032101 (2019); <https://doi.org/10.1063/1.5108790>

Submitted: 02 May 2019 . Accepted: 26 June 2019 . Published Online: 15 July 2019

A. Y. Polyakov, In-Hwan Lee , N. B. Smirnov , E. B. Yakimov , I. V. Shchemerov, A. V. Chernykh , A. I. Kochkova, A. A. Vasilev, F. Ren , P. H. Carey , and S. J. Pearton 



View Online



Export Citation



CrossMark

## ARTICLES YOU MAY BE INTERESTED IN

[Anisotropic etching of  \$\beta\$ -Ga<sub>2</sub>O<sub>3</sub> using hot phosphoric acid](#)

Applied Physics Letters **115**, 013501 (2019); <https://doi.org/10.1063/1.5093188>

[Low-temperature behaviors of multilayer MoS<sub>2</sub> transistors with ohmic and Schottky contacts](#)

Applied Physics Letters **115**, 033501 (2019); <https://doi.org/10.1063/1.5099380>

[A review of Ga<sub>2</sub>O<sub>3</sub> materials, processing, and devices](#)

Applied Physics Reviews **5**, 011301 (2018); <https://doi.org/10.1063/1.5006941>

## Applied Physics Letters

Mid-IR and THz frequency combs  
special collection

[Read Now!](#)

AIP  
Publishing

# Hydrogen plasma treatment of $\beta$ -Ga<sub>2</sub>O<sub>3</sub>: Changes in electrical properties and deep trap spectra

Cite as: Appl. Phys. Lett. **115**, 032101 (2019); doi: [10.1063/1.5108790](https://doi.org/10.1063/1.5108790)

Submitted: 2 May 2019 · Accepted: 26 June 2019 ·

Published Online: 15 July 2019



View Online



Export Citation



CrossMark

A. Y. Polyakov,<sup>1</sup> In-Hwan Lee,<sup>2</sup> N. B. Smirnov,<sup>1</sup> E. B. Yakimov,<sup>1,3</sup> I. V. Shchemerov,<sup>1</sup> A. V. Chernykh,<sup>1</sup> A. I. Kochkova,<sup>1</sup> A. A. Vasilev,<sup>1</sup> F. Ren,<sup>4</sup> P. H. Carey IV,<sup>4</sup> and S. J. Pearton<sup>5,a)</sup>

## AFFILIATIONS

<sup>1</sup>National University of Science and Technology MISiS, 4 Leninskiy Ave., Moscow 119049, Russia

<sup>2</sup>Department of Materials Science and Engineering, Korea University, Seoul 02841, South Korea

<sup>3</sup>Institute of Microelectronics Technology and High Purity Materials, Russian Academy of Science, 6 Academician Ossipyan str., Chernogolovka, Moscow Region 142432, Russia

<sup>4</sup>Department of Chemical Engineering, University of Florida, Gainesville, Florida 32611, USA

<sup>5</sup>Department of Materials Science and Engineering, University of Florida, Gainesville, Florida 32611 USA

<sup>a)</sup>Author to whom correspondence should be addressed: [spear@mse.ufl.edu](mailto:spear@mse.ufl.edu)

## ABSTRACT

The effects of hydrogen plasma treatment of  $\beta$ -Ga<sub>2</sub>O<sub>3</sub> grown by halide vapor phase epitaxy and doped with Si are reported. Samples subjected to H plasma exposure at 330 °C developed a wide ( $\sim 2.5 \mu\text{m}$ -thick) region near the surface, depleted of electrons at room temperature. The thickness of the layer is in reasonable agreement with the estimated hydrogen penetration depth in  $\beta$ -Ga<sub>2</sub>O<sub>3</sub> based on previous deuterium profiling experiments. Admittance spectroscopy and photoinduced current transient spectroscopy measurements place the Fermi level pinning position in the H treated film near  $E_c - 1.05 \text{ eV}$ . Annealing at 450 °C decreased the thickness of the depletion layer to  $1.3 \mu\text{m}$  at room temperature and moved the Fermi level pinning position to  $E_c - 0.8 \text{ eV}$ . Further annealing at 550 °C almost restored the starting shallow donor concentration and the spectra of deep traps dominated by  $E_c - 0.8 \text{ eV}$  and  $E_c - 1.05 \text{ eV}$  observed before hydrogen treatment. It is suggested that hydrogen plasma exposure produces surface damage in the near-surface region and passivates or compensates shallow donors.

Published under license by AIP Publishing. <https://doi.org/10.1063/1.5108790>

$\beta$ -Ga<sub>2</sub>O<sub>3</sub> is of great current interest because of the prospects for use in next generation high-power electronics and solar-blind photodetectors.<sup>1–3</sup> Recent advances in bulk growth have allowed realization of large diameter, high quality crystals, and substrates prepared by edge-defined film-fed growth (EFG) are commercially available, both n-type and semi-insulating.<sup>4</sup> Good quality epitaxial films with n-type conductivity have been demonstrated for various growth techniques, particularly for halide vapor phase epitaxy (HVPE), for which films on native substrates have been commercialized.<sup>1–4</sup> Ternary solid solutions of (Al<sub>x</sub>Ga<sub>1–x</sub>)<sub>2</sub>O<sub>3</sub> compatible with binary Ga<sub>2</sub>O<sub>3</sub> have been developed for use in high electron mobility transistor (HEMT) applications.<sup>5</sup> Advances in Ohmic contact preparation, Schottky diode fabrication, and dielectric film deposition have been reported.<sup>1–3</sup> However, issues remain; among them is the behavior of various impurities in  $\beta$ -Ga<sub>2</sub>O<sub>3</sub>.

In this letter, we report the effects of hydrogen plasma exposure on the near-surface properties of Ga<sub>2</sub>O<sub>3</sub>. Theory suggests that hydrogen is a shallow donor with low formation energy in Ga<sub>2</sub>O<sub>3</sub>.<sup>6,7</sup>

Hydrogen complexes with oxygen vacancies are also expected to be shallow donors.<sup>6</sup> Experimental studies have been mainly concerned with hydrogen introduced during high temperature anneals in H<sub>2</sub> or <sup>2</sup>H<sub>2</sub>.<sup>8–12</sup> IR absorption peaks observed at  $3437 \text{ cm}^{-1}$  in annealed samples by Weiser *et al.*<sup>10</sup> are attributed to a gallium vacancy decorated with two hydrogen atoms. Ritter *et al.*<sup>12</sup> demonstrated that hydrogen-annealing of Ga<sub>2</sub>O<sub>3</sub>:Mg produced an IR peak at  $3492 \text{ cm}^{-1}$ , assigned to an O-H bond-stretching mode of a neutral MgH complex. Ingebrigtsen *et al.*<sup>13</sup> found that proton irradiation produced severe reductions in the carrier concentration above threshold doses and that passivation of gallium vacancies played a role in the thermal recovery characteristics. Von Bardeleben *et al.*<sup>14</sup> reported that proton irradiation introduces two main paramagnetic defects in  $\beta$ -Ga<sub>2</sub>O<sub>3</sub>, stable at room temperature. Hydrogen accumulation at the surface causes upwards band bending.<sup>8</sup>

A question remains as to whether hydrogen behaves in Ga<sub>2</sub>O<sub>3</sub> as it often does in other semiconductors, i.e., forms neutral complexes

with shallow donors or with deep level defects, thus passivating them.<sup>11</sup> One approach to check this is by introducing hydrogen (or deuterium) from plasmas. Initial work where deuterium diffusion in  $\beta$ -Ga<sub>2</sub>O<sub>3</sub> treated in D<sub>2</sub> plasma at 100–270 °C was studied by secondary ion mass spectrometry (SIMS) profiling<sup>15</sup> showed concentration profiles with characteristic plateaus often associated with the formation of hydrogen/deuterium complexes with defects and dopants.<sup>11</sup> The depth of the D diffusion increased from 0.2  $\mu$ m for 100 °C to 0.6  $\mu$ m for 270 °C for a fixed deuteration time of 0.5 h.<sup>15</sup> Annealing at 400 °C decreased the D concentration on the plateau and the spatial extent of the plateau region, suggesting partial breakup of complexes and D out-diffusion (see also Ref. 16). However, no direct information on the changes induced by the formation and dissociation of such complexes on electrical properties was reported. In this letter, we discuss the results of hydrogen plasma exposure on near-surface electrical properties.

The samples were from Tamura Corp. (Japan). The epitaxial layers were grown by HVPE on bulk n<sup>+</sup> substrates prepared by EFG.<sup>4</sup> The thickness of the films was 10  $\mu$ m, and they were doped with Si and had (010) orientation. The growth was performed at temperatures near 1000 °C, with the growth rate of 4–5  $\mu$ m/h, using silane for Si doping. The wafers were cut into several pieces, some of which were kept as reference samples, while others were treated for 1 h at 330 °C in RF 13.56 MHz H plasmas.<sup>15</sup> These H plasma exposed samples were studied directly after treatment (H plasma sample below) and after rapid thermal annealing in N<sub>2</sub> for 5 min at 450 °C (H plasma 450 °C sample) and 550 °C (H plasma 550 °C sample). For all samples, full-area back Ohmic contacts were prepared before H plasma treatment by deposition of Ti/Ni thin films on Ar plasma treated and annealed surfaces of n<sup>+</sup> substrates.<sup>16</sup> Ni Schottky diodes, 1 mm in diameter, were prepared by e-beam deposition at room temperature. This allowed avoidance of high temperature treatments after H plasma exposure.

Characterization consisted of capacitance vs voltage, C-f measurements at frequencies from 20 Hz to 1 MHz, capacitance-voltage (C-V) profiling at different frequencies, admittance spectra (AS),<sup>17</sup> deep level transient spectroscopy (DLTS),<sup>18</sup> current DLTS (CDLTS),<sup>18</sup> and photoinduced current transient spectroscopy (PICTS)<sup>19</sup> in the temperature range of 77–500 K. Diffusion length  $L_d$  of nonequilibrium charge carriers was measured at 300 K by monitoring electron beam induced current (EBIC) collection efficiency on the probing electron beam energy of the scanning electron microscope (SEM).<sup>20–22</sup>

Before H plasma exposure, the reference sample capacitance at 300 K was 650 pF, independent of frequency (Fig. 1), and C-V profiling up to –5 V yielded the net shallow donor concentration of  $N_d = 2 \times 10^{17} \text{ cm}^{-3}$ . No significant capacitance freeze out was detected, suggesting that the donors were shallow. DLTS spectra showed two major peaks belonging to electron traps with levels near  $E_c - 0.8 \text{ eV}$  and  $E_c - 1.05 \text{ eV}$ , with signatures close to those of the electron traps E2\* and E3.<sup>23–25</sup> Figure 2 shows the spectra obtained with a reverse bias of –5 V pulsed to 0 V for 3 s for DLTS time windows  $t_1/t_2 = 1.75 \text{ s}/17.5 \text{ s}$ . The y-axis in the figure represents the DLTS signal  $\Delta C/C$  multiplied by  $2N_d$  and divided by the DLTS spectrometer function  $F = \exp(-t_2/\tau) - \exp(-t_1/\tau)$ , with  $\tau = (t_2 - t_1)/\ln(t_2/t_1)$ .<sup>18</sup> The convention is that positive peaks correspond to electron traps (capacitance increases during the capacitance transient<sup>18</sup>). At temperatures corresponding to the peaks, the peak magnitude is equal to the trap concentration

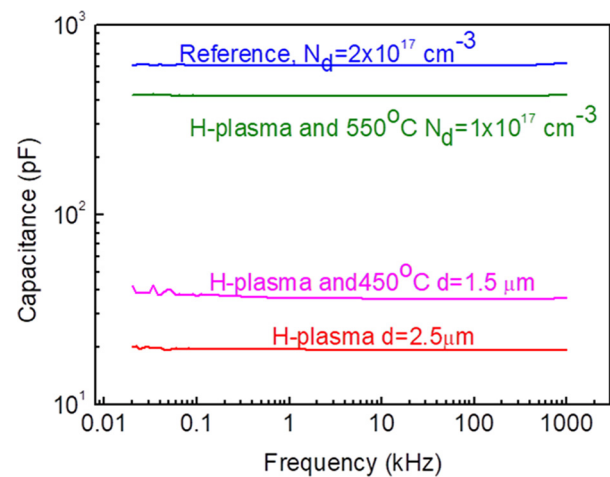


FIG. 1. Room temperature C-f dependences before and after plasma treatment and after subsequent annealing.

without the  $\lambda$ -correction.<sup>18</sup> With such correction, the E2\* and E3 trap concentrations were  $5.4 \times 10^{15} \text{ cm}^{-3}$  and  $1.7 \times 10^{15} \text{ cm}^{-3}$ .

The diffusion length ( $L_d$ ) of nonequilibrium charge carriers in EBIC was estimated from the dependence on probing electron beam energy  $E_b$  as 110 nm for the reference sample. The dependence of collection efficiency of the EBIC current is shown as a function of beam accelerating voltage in Fig. 3.  $L_d$  estimated after hydrogen treatment was 50 nm, with a low collection efficiency in the space charge region (the peak in the curve) because of the strong recombination induced by defects. After annealing at 450 °C, the diffusion length was 70 nm, and after 550 °C, it was 80 nm. The donor concentration and the E2\* and E3 trap concentrations in the reference sample were an order of magnitude higher than in HVPE films studied by us previously,<sup>20,24,25</sup> which correlates with the lower  $L_d$  in the reference sample compared to previously reported for HVPE  $\beta$ -Ga<sub>2</sub>O<sub>3</sub> [ $L_d \sim 450 \text{ nm}$  (Refs. 20, 24, and 25)].

After H plasma treatment, the sample capacitance at 300 K decreased to 19.7 pF, independent of frequency or voltage. This suggests that, at 300 K, the top 2.5  $\mu$ m portion of the film was essentially

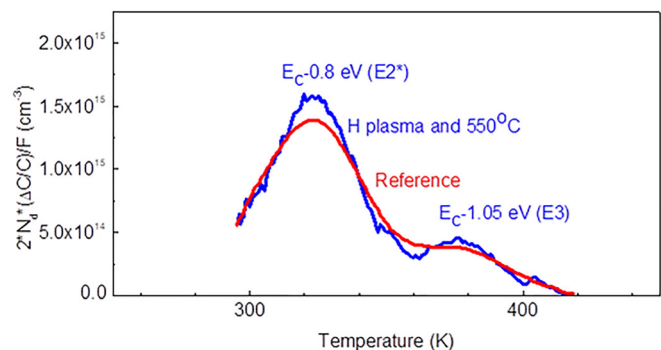
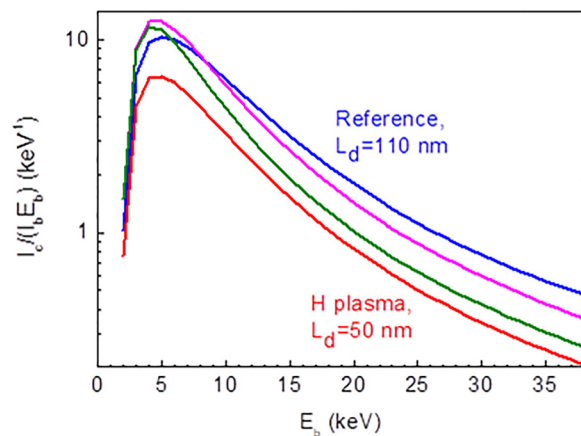


FIG. 2. DLTS spectra measured for the reference sample (red curve) and after H plasma and 550 °C anneal (blue curve); measurements at –5 V, pulsed to 0 V for 3 s, and time windows  $t_1/t_2 = 1.75 \text{ s}/17.5 \text{ s}$ .



**FIG. 3.** The dependence of collection efficiency of the EBIC current  $I_c$  as a function of the beam accelerating voltage  $E_b$ . This efficiency is measured as the ratio  $I_c/(I_b E_b)$ , where  $I_b$  is the probing beam current. Only the results of fitting are shown, not the actual experimental points for each sample.

bereft of centers that could contribute to capacitance for probing frequencies in the range of 20 Hz–1 MHz, i.e., such centers for which their occupation with electrons could follow the frequency in C-V measurements.<sup>17,18</sup> Thus, the entire thickness of this part of the film behaved at 300 K as a dielectric layer with a thickness of 2.5  $\mu\text{m}$ . The thickness is close to the expected hydrogen penetration depth when considering previous deuterium profiling experiments,<sup>15</sup> and taking into account that we used hydrogen instead of deuterium, our treatment temperature was 330 °C rather than 270 °C and the treatment time was twice as long.<sup>15</sup>

Annealing at 450 °C decreased the thickness of this layer to 1.3  $\mu\text{m}$ . Further annealing at 550 °C rendered the hydrogen treated top portion of the film conducting again, with the net donor density deduced from 300 K C-V profiling almost the same as before hydrogen treatment,  $10^{17} \text{ cm}^{-3}$ . DLTS measurements on this 550 °C annealed sample showed deep electron traps similar in energy and concentration to those in the pristine state. DLTS was not suitable for measurements on the as-hydrogenated sample and after 450 °C annealing because of the high series resistance of these films. Some information on the presence of deep centers could be gleaned from high-temperature/low-frequency admittance spectra measurements and from PICTS measurements, as demonstrated for semi-insulating  $\beta\text{-Ga}_2\text{O}_3$  doped with Fe or Mg.<sup>26–28</sup>

If the Fermi level in the hydrogenated samples was pinned at deep centers, the static space charge region width would be determined by the concentration of centers that preserved their electrons.<sup>26–28</sup> These centers would contribute to capacitance,  $C$ , and AC conductance,  $G$ , at high temperatures and low frequencies at which the centers can follow the probing electric field in admittance.<sup>26–28</sup> Thus, one would expect capacitance to increase with increasing temperature and decreasing frequency, until it reaches values corresponding to the depletion width determined by the concentration of uncompensated deep centers pinning the Fermi level. These steps in capacitance should shift to higher temperatures with increasing frequency. In conductance, one expects the corresponding peaks whose temperature also shifts to higher values with increasing frequency.

This shift of the peak/step temperature can be used to calculate the depth of the level and the electron capture cross section from the condition  $e_n = \omega = 2\pi f$ , where  $e_n$  is the emission rate from the deep center,  $\omega$  is the angular frequency, and  $f$  is the frequency in admittance measurements.<sup>17,18</sup>

If C-V measurements are done at frequencies/temperatures where the step in capacitance is observed, one can calculate the concentration of electrons on the deep levels producing the step.<sup>26–28</sup> Such sets of steps in capacitance/peaks in conductance could be observed in the as-hydrogenated sample and the sample annealed at 450 °C. Figure 4(a) shows the temperature dependence of capacitance for the as-hydrogenated sample for several low frequencies, while Fig. 4(b) shows respective peaks in conductance [conductance in Fig. 4(b) is divided by the angular frequency  $\omega = 2\pi f$  (Refs. 17 and 18)]. The depth of the level is 1.05 eV, with a capture cross section of  $2 \times 10^{-13} \text{ cm}^2$ , close to the parameters of the E3 traps in the starting sample. The concentration of traps determined from C-V profiling at 20 Hz was  $7 \times 10^{15} \text{ cm}^{-3}$ . The width of the space charge region at  $-5 \text{ V}$  was 0.3  $\mu\text{m}$ . After 450 °C annealing, the Fermi level was pinned on the trap with an energy level of 0.75 eV and a capture cross section

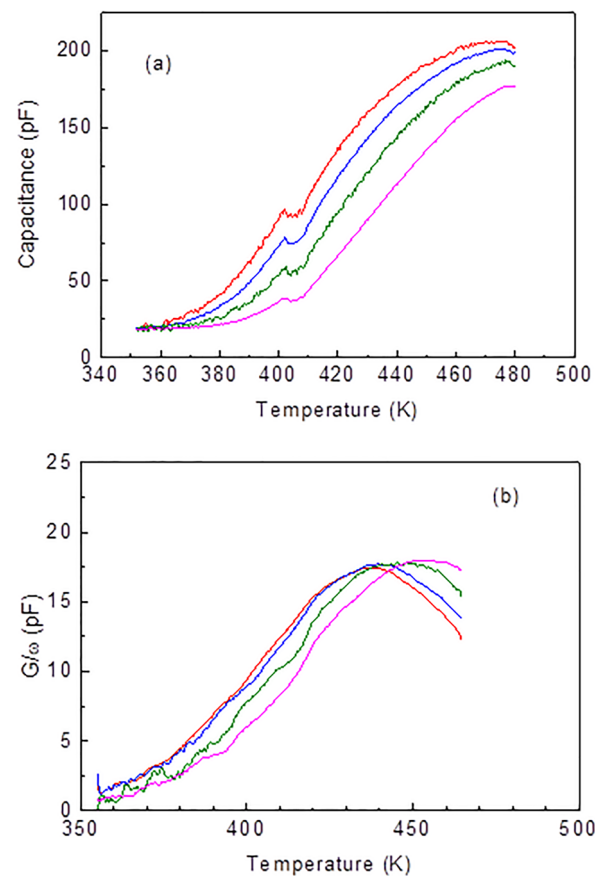


**FIG. 4.** (a) Capacitance vs temperature measured for sample treated in H plasma for frequencies 25 Hz (red curve), 30 Hz (blue curve), 45 Hz (olive curve), and 70 Hz (magenta curve); (b)  $G/\omega$  temperature dependence for the same set of frequencies; measurements at  $-5 \text{ V}$ .



for electrons of  $1.2 \times 10^{-15} \text{ cm}^2$ , not far from the signature of the  $E_2^*$  center. The density of electrons on these traps from high-temperature/low-frequency C-V profiling was  $2.3 \times 10^{16} \text{ cm}^{-3}$ . For both centers, their concentration is several times higher than that obtained before H treatment.

Proton irradiation increases the density of the  $E_2$  and  $E_3$  electron traps,<sup>16,25</sup> and so it cannot be ruled out that these centers can contain hydrogen as a constituent. However, the steady increase in the centers' density with proton fluence suggests involvement of native point defects. Therefore, hydrogen plasma treatment damage could have promoted the additional formation of such native defects, at least in the upper  $\sim 0.3 \mu\text{m}$  of the sample. Our measurements of the effects of dense Ar plasma treatment on deep traps in HVPE  $\beta\text{-Ga}_2\text{O}_3$  films show that such treatment can stimulate the increase in concentration of  $E_2^*$  and  $E_3$  traps in the near surface region ( $\sim 0.2 \mu\text{m}$ ). However, in the absence of passivation or compensation of shallow donors in the rest of the film, this increased density of surface deep traps would lead to a decrease in the apparent contact voltage of the Schottky diode, as in Ar plasma treated samples, not to the layer becoming an insulator at room temperature, as for H treated samples. This suggests that either shallow Si donors in the bulk of hydrogenated films are passivated or compensated or that with hydrogen plasma treatment, the width of the damaged region with a high density of deep traps is thicker than with Ar plasmas.

The density of  $E_2^*$  and  $E_3$  traps detected in admittance measurements is, even for the near surface region, too low to account for compensation of shallow donors with a density of  $2 \times 10^{17} \text{ cm}^{-3}$ , as in the starting material. Then, one requires either formation of deeper acceptors with high density throughout the thickness of the H treated portion of the film or, more likely, hydrogen passivation of shallow Si donors. Indeed, the density of deep acceptors should be over  $10^{17} \text{ cm}^{-3}$ , to render the hydrogenated portion of the film highly resistive. With these densities, such acceptors should be detectable in low frequency, high temperature C-V measurements with illumination.<sup>25,26</sup> The most likely candidates seem to be deep acceptors with the optical ionization threshold near 2.3 eV and 3.4 eV.<sup>25,26,29</sup> Their presence in very high concentration is not confirmed in our high temperature/low frequency C-V measurements with illumination. The proposed hydrogen passivation of donors would be in contrast to theoretical predictions and to some experimental results obtained for H introduction at high temperatures during growth.<sup>6–8</sup>

Note that the Fermi level in the H treated sample is pinned near  $E_c\text{-}1.05 \text{ eV}$ , suggesting this trap to be the main uncompensated deep center. This is opposite to that observed in DLTS on reference samples and  $550^\circ\text{C}$  annealed samples where the  $E_2^*$  ( $E_c\text{-}0.8 \text{ eV}$ ) trap is the major deep center. The Fermi level is shifted to  $E_c\text{-}0.75 \text{ eV}$  after annealing at  $450^\circ\text{C}$ . The latter could be either the result of the shallow donor concentration increasing with annealing, thus shifting the Fermi level upwards, or due to the  $E_c\text{-}1.05 \text{ eV}$  traps being more susceptible to annealing than the  $E_c\text{-}0.75 \text{ eV}$  defects, causing repumping of defects upon annealing from the deeper centers to the shallower centers. PICTS spectra measurements summarized in Fig. 5 favor the latter. PICTS measurements were done with below-bandgap excitation with high-power 3.4 eV light (250 mW 365 nm wavelength GaN-based light emitting diodes (LEDs) providing essentially bulk excitation). For the as-hydrogenated samples, the spectra were dominated by a prominent peak belonging to a trap with an energy level of  $E_c\text{-}$

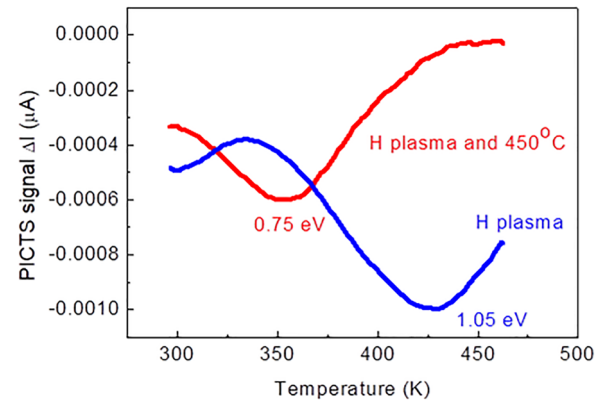


**FIG. 5.** PICTS spectra measured for the H plasma treated sample (blue curve) and H plasma treated sample annealed at  $450^\circ\text{C}$  (red curve); measurements at  $-10 \text{ V}$ , excitation with 3.4 eV high-power LED (pulse 5 s), and time windows 60 ms/600 ms.

$1.05 \text{ eV}$  and an electron capture cross section of  $\sim 7.3 \times 10^{-14} \text{ cm}^2$ , most likely the  $E_3$  trap. There is little evidence of a signal from a shallower trap near  $E_c\text{-}0.75 \text{ eV}$ . After  $450^\circ\text{C}$  annealing, the situation is reversed. Now the dominant signal comes from the  $E_c\text{-}0.75 \text{ eV}$  trap with a very weak signal from the  $E_c\text{-}1.05 \text{ eV}$  center.

Diffusion lengths in the reference and  $550^\circ\text{C}$  annealed samples were reasonably close, 110 nm and 80 nm, respectively, which correlates with the deep electron trap type and concentration being almost the same. The slightly lower diffusion length measured for the  $550^\circ\text{C}$  sample could be due to the lower charge carrier mobility and residual surface damage decreasing the collection efficiency. For the hydrogen treated sample, the low diffusion length was both due to a decrease in the lifetime of charge carriers because of the higher concentration of the deep traps and due to additional charge capture in the hydrogenated layer equivalent to a decreased effective mobility of charge carriers. Micro-cathodoluminescence (MCL) spectra measurements also point to a decreased lifetime after treatment. Room temperature MCL spectra before H treatment were dominated by the usual broadband extending from  $\sim 300 \text{ nm}$  to  $\sim 550 \text{ nm}$  common for HVPE  $\beta\text{-Ga}_2\text{O}_3$ .<sup>24</sup> After the H plasma treatment, the band was the same, but the intensity was 2 times lower for near-surface excitation (probing beam energy 3 keV), reflecting the decreased lifetime in the H treated sample.

Thus, in hydrogen plasma treated HVPE n-type films of  $\beta\text{-Ga}_2\text{O}_3$  (Si), we observed a pronounced decrease in the concentration of shallow donors that provide free electrons, which does not corroborate the theoretical prediction that hydrogen in  $\beta\text{-Ga}_2\text{O}_3$  should be an efficient shallow donor. There is the possibility that hydrogen forms electrically active complexes with deep native defects, such as Ga vacancies,<sup>11,14</sup> and gives rise to donor compensation, but C-V profiling experiments with monochromatic illumination do not indicate high densities of deep acceptor concentration before or after hydrogen treatment, certainly not  $\sim 10^{17} \text{ cm}^{-3}$  necessary to compensate the starting n-type conductivity. It appears more likely that hydrogen introduced from H plasmas forms neutral complexes, thus passivating donors as in other semiconductors.<sup>9</sup> We see evidence that hydrogen treatment can enhance the concentration of the main deep donors with levels near  $E_c\text{-}0.8 \text{ eV}$  ( $E_2^*$  traps) and  $E_c\text{-}1.05 \text{ eV}$  ( $E_3$  traps), which would imply that these traps could be complexes of native defects and

hydrogen of the kind observed in localized vibrational mode (LVM) spectroscopy.<sup>9</sup> Why the behavior of hydrogen introduced during high temperature growth and in low temperature plasma treatment is different needs additional experiments. A final comment can be made on how hydrogen might affect undoped Ga<sub>2</sub>O<sub>3</sub>. We speculate that this would depend on the doping level since the hydrogen penetration depth will depend on the charge state of diffusing hydrogen, determined by the starting Fermi level position, the density of defects produced by plasma treatment (hydrogen penetration is much smaller for treatment under mild plasma conditions), the actual density of shallow donors and of compensating deep acceptors, and finally on whether free hydrogen expected to produce shallow donors remains after the hydrogen plasma treatment.

The work at NUST MISiS was supported in part by the Russian Science Foundation, grant no. 19-19-00409. The work at IMT RAS was supported by the State Task No. 075-00475-19-00. The work at UF was sponsored by the Department of the Defense, Defense Threat Reduction Agency, HDTRA1-17-1-011, monitored by Jacob Calkins and also by NSF DMR 1856662 (Tania Paskova).

## REFERENCES

- <sup>1</sup>S. J. Pearton, J. Yang, P. H. Cary, F. Ren, J. Kim, M. J. Tadjer, and M. A. Mastro, *Appl. Phys. Rev.* **5**, 011301 (2018).
- <sup>2</sup>M. A. Mastro, A. Kuramata, J. Calkins, J. Kim, F. Ren, and S. J. Pearton, *ECS J. Solid State Sci. Technol.* **6**, P356 (2017).
- <sup>3</sup>Z. Galazka, *Semicond. Sci. Technol.* **33**, 113001 (2018).
- <sup>4</sup>See [www.tamura-ss.co.jp/en/products](http://www.tamura-ss.co.jp/en/products) for details on the substrates and epitaxial layers of gallium oxide commercially available.
- <sup>5</sup>Y. Zhang, C. Joishi, Z. Xia, M. Brenner, S. Lodha, and S. Rajan, *Appl. Phys. Lett.* **112**, 233503 (2018).
- <sup>6</sup>J. B. Varley, J. R. Weber, A. Janotti, and C. G. Van de Walle, *Appl. Phys. Lett.* **97**, 142106 (2010).
- <sup>7</sup>J. B. Varley, H. Peelaers, A. Janotti, and C. G. Van de Walle, *J. Phys.: Condens. Matter* **23**, 334212 (2011).
- <sup>8</sup>J. E. N. Swallow, J. B. Varley, L. A. H. Jones, J. T. Gibbon, L. F. J. Piper, V. R. Dhanak, and T. D. Veal, *APL Mater.* **7**, 022528 (2019).
- <sup>9</sup>M. Stavola, W. B. Fowler, Y. Qin, P. Weiser, and S. J. Pearton, in *Ga<sub>2</sub>O<sub>3</sub>, Technology, Devices and Applications*, edited by S. J. Pearton, F. Ren, and M. Mastro (Elsevier, Amsterdam, 2018), Chap. IX, p. 191.
- <sup>10</sup>P. Weiser, M. Stavola, W. B. Fowler, Y. Qin, and S. J. Pearton, *Appl. Phys. Lett.* **112**, 232104 (2018).
- <sup>11</sup>Y. Qin, M. Stavola, W. B. Fowler, P. Weiser, and S. J. Pearton, *ECS J. Solid State Sci. Technol.* **8**, Q3103 (2019).
- <sup>12</sup>J. R. Ritter, J. Huso, P. T. Dickens, J. B. Varley, K. G. Lynn, and M. D. McCluskey, *Appl. Phys. Lett.* **113**, 052101 (2018).
- <sup>13</sup>M. E. Ingebrigtsen, A. Yu. Kuznetsov, B. G. Svensson, G. Alfieri, A. Mihaila, U. Badstübner, A. Perron, L. Vines, and J. B. Varley, *APL Mater.* **7**, 022510 (2019).
- <sup>14</sup>H. J. von Bardeleben, S. Zhou, U. Gerstmann, D. Skachkov, W. R. L. Lambrecht, Q. D. Ho, and P. Deák, *APL Mater.* **7**, 022521 (2019).
- <sup>15</sup>R. Sharma, E. Patrick, M. E. Law, S. Ahn, F. Ren, S. J. Pearton, and A. Kuramata, *ECS J. Solid State Sci. Technol.* **6**, P794 (2017).
- <sup>16</sup>A. A. Talukder, J. Pokharel, M. Shrestha, and Q. H. Fan, *J. Appl. Phys.* **120**, 155303 (2016).
- <sup>17</sup>L. Pautrat, B. Katircioglu, N. Magnea, D. Bensahel, J. C. Pfister, and L. Revoil, *Solid-State Electron.* **23**, 1159 (1980).
- <sup>18</sup>D. K. Schroeder, *Semiconductor Material and Device Characterization* (John Wiley and Sons, New York, 1990), p. 587.
- <sup>19</sup>M. Tapiero, N. Benjelloun, J. P. Zielinger, S. El Hamd, and C. Noguét, *J. Appl. Phys.* **64**, 4006 (1988).
- <sup>20</sup>E. B. Yakimov, A. Y. Polyakov, N. B. Smirnov, I. V. Shchemerov, J. Yang, F. Ren, G. Yang, J. Kim, and S. J. Pearton, *J. Appl. Phys.* **123**, 185704 (2018).
- <sup>21</sup>A. Y. Polyakov, N. B. Smirnov, I.-H. Lee, and S. J. Pearton, *J. Vac. Sci. Technol., B* **33**, 061203 (2015).
- <sup>22</sup>A. Y. Polyakov, N. B. Smirnov, I. V. Shchemerov, D. Gogova, S. A. Tarelkin, I.-H. Lee, and S. J. Pearton, *ECS J. Solid State Sci. Technol.* **7**, P260 (2018).
- <sup>23</sup>M. E. Ingebrigtsen, J. B. Varley, A. Yu. Kuznetsov, B. G. Svensson, G. Alfieri, A. Mihaila, U. Badstübner, and L. Vines, *Appl. Phys. Lett.* **112**, 042104 (2018).
- <sup>24</sup>A. Y. Polyakov, N. B. Smirnov, I. V. Shchemerov, S. J. Pearton, F. Ren, A. V. Chernykh, P. B. Lagov, and T. V. Kulevoy, *APL Mater.* **6**, 096102 (2018).
- <sup>25</sup>A. Y. Polyakov, N. B. Smirnov, I. V. Shchemerov, E. B. Yakimov, S. J. Pearton, C. Fares, J. Yang, F. Ren, J. Kim, P. B. Lagov, V. S. Stolbunov, and A. Kochkova, *Appl. Phys. Lett.* **113**, 092102 (2018).
- <sup>26</sup>A. Y. Polyakov, N. B. Smirnov, I. V. Shchemerov, S. J. Pearton, F. Ren, A. V. Chernykh, and A. I. Kochkova, *Appl. Phys. Lett.* **113**, 142102 (2018).
- <sup>27</sup>A. Y. Polyakov, N. B. Smirnov, I. V. Shchemerov, A. V. Chernykh, E. B. Yakimov, A. I. Kochkova, A. N. Tereshchenko, and S. J. Pearton, *ECS J. Solid State Sci. Technol.* **8**, Q3091 (2019).
- <sup>28</sup>A. Y. Polyakov, N. B. Smirnov, I. V. Shchemerov, E. B. Yakimov, S. J. Pearton, F. Ren, A. V. Chernykh, D. Gogova, and A. I. Kochkova, *ECS J. Solid State Sci. Technol.* **8**, Q3019 (2019).
- <sup>29</sup>H. Gao, S. Muralidharan, N. Pronin, Md. R. Karim, S. M. White, T. Asel, G. Foster, S. Krishnamoorthy, S. Rajan, L. R. Cao, M. Higashiwaki, H. von Wenckstern, M. Grundmann, H. Zhao, D. C. Look, and L. J. Brillson, *Appl. Phys. Lett.* **112**, 242102 (2018).